

Internodal Distance Distributions for Static and Mobile Nodes in 2D/3D Wireless Networks

Nicholas Vaiopoulos, Alexander Vavoulas, Harilaos G. Sandalidis, Konstantinos K. Delibasis, and Dimitris Varoutas

Abstract—This letter presents a unified analytical framework for internodal distance distributions in 2D and 3D wireless networks, with nodes confined to concentric circular or spherical regions. Four deployment scenarios are considered, covering all combinations of static (uniform) and mobile (random waypoint-based) nodes. For each scenario, closed-form expressions for the internodal distance probability density functions are derived, incorporating both geometric constraints and spatial effects introduced by mobility. Equal-radius cases are also addressed. Beta-distribution approximations and Monte Carlo simulations demonstrate the accuracy and validity of the analytical results.

Index Terms—Wireless networks, internodal distance distributions, random location, mobility.

I. INTRODUCTION

INTERNODAL distance distributions are particularly critical in random networks, where node positions are determined by stochastic models [1]. These models are commonly employed to characterize wireless environments, such as mobile ad hoc networks (MANETs), wireless sensor networks (WSNs), vehicular networks, and emerging systems like UAV swarms and three-dimensional (3D) Internet of Things (IoT) deployments [2]. In these systems, randomness often stems from unpredictable node placement, user mobility, and environmental factors. Accurate knowledge of internodal distributions is essential for the effective analysis and design of wireless communication protocols, including routing, resource allocation, power control, and capacity planning [3].

Different spatial and mobility models can produce significantly varying distance distributions. For example, uniform random node placement generally results in symmetric, well-understood distributions, while mobility models such as random waypoint (RWP) or Gauss-Markov lead to nonuniform, often center-biased spatial densities. As wireless networks evolve to include static infrastructure, mobile users, and aerial platforms, accounting for this spatial diversity becomes increasingly important. Therefore, a comprehensive understanding of distance distributions under various geometric and stochastic assumptions is crucial for realistic modeling and effective network design.

Recent studies have investigated 3D internodal distance models for various deployment scenarios, including hexagonal, conical, and spherical volumes, driven by applications in

UAV, satellite, and underwater communication systems [4]–[7]. Beta-type approximations are commonly used for bounded regions [8], though they often fail to account for non-uniform spatial effects or mobility-induced variations. Nichols *et al.* in [9], analyzed uniform 3D deployments, while mobility effects have been explored using random walk (RW) and RWP models [10]. Zhong *et al.* [11] derived integral-form probability density function (PDFs) and cumulative distribution function (CDFs) of distances for static–mobile node pairs in two-dimensional (2D) domains, but extensions to other scenarios and higher-dimensional geometries remain limited.

Existing studies primarily rely on simulations or approximate statistics rather than unified analytical formulations to address diverse spatial and mobility configurations [12]. In this work, we introduce a novel analytical framework that provides exact closed-form expressions for internodal distance distributions across all four node-pair combinations (static-static, static-mobile, mobile-static, and mobile-mobile) in both 2D and 3D environments, under uniform and RWP-based spatial models.

II. MODEL ASSUMPTIONS

In the 2D case, we consider two nodes constrained within concentric circular regions of radii R_1 and R_2 , where $R_1 < R_2$. This framework is naturally extended to 3D by substituting the circular regions with concentric spherical regions of identical radii. Nodes are either uniformly distributed within their respective regions or exhibit mobility according to the RWP model. Under these assumptions, four representative user distribution scenarios are defined for both 2D and 3D environments:

- **Scenario 1 (s1):** The mobile node lies within a circular (or spherical) region of radius R_1 and the static node within radius R_2 .
- **Scenario 2 (s2):** The static node is confined to a radius R_1 and the mobile node to a radius R_2 .
- **Scenario 3 (s3):** Both nodes are mobile, each confined within regions of radii R_1 and R_2 , respectively.
- **Scenario 4 (s4):** Both nodes are static within regions of radii R_1 and R_2 , respectively, as examined in [13] for the 2D case only.

A special case with $R_1 = R_2$ is also considered, as studied in several 2D and 3D scenarios in [11], [14], and [15]. Under these assumptions, the analytical expression for the PDF of the internodal distance, r , is obtained as

$$f_{\mathbf{r}}(r) = \int_0^\infty f_{\mathbf{r}/\rho}(r/\rho) f_{\rho}(\rho) d\rho, \quad (1)$$

Nicholas Vaiopoulos, Alexander Vavoulas, Harilaos G. Sandalidis, and Konstantinos K. Delibasis are with the Department of Computer Science and Biomedical Informatics, University of Thessaly, Papasiopoulou 2-4, 35131, Lamia, Greece. e-mail: {nvaio,vavoulas,sandalidis,kdelimpasis}@dib.uth.gr.

Dimitris Varoutas is with the Department of Informatics and Telecommunications, University of Athens, Panepistimiopolis, 15784, Athens, Greece. e-mail: arkas@di.uoa.gr.

where $f_{r/\rho}(r/\rho)$ denotes the conditional PDF of r , given that node 1 is located at a distance ρ from the center. The term $f_\rho(\rho)$ represents the PDF of the distance of node 1, corresponding either to the RWP model or a uniform distribution, depending on the scenario under consideration. The explicit expressions for these distributions are provided in Table II for the 2D case and Table V for the 3D case.

To compute $f_{r/\rho}(r/\rho)$, it is assumed that node 2 is located on a circular ring or spherical shell of radius r centered at node 1. Only the portion of this ring or shell which is enclosed in the disk or sphere of radius R_2 contributes to the conditional probability. Depending on the relative values of r , ρ , R_1 , and R_2 , this region may be fully contained within, partially overlap with, or lie outside the corresponding disk or sphere. Table I specifies the three intervals of r over which the conditional probability takes distinct forms, along with the corresponding integration limits in (1). These intervals are defined as follows.

- **Interval I** ($0 < r < R_-$): The circular ring or spherical shell (dashed line in Table I) is fully contained within the disk/sphere of radius R_2 for all ρ . Therefore, $g_1(\rho, r)$ is used¹.
- **Interval II** ($R_- < r < R_2$): The ring or shell is fully contained within the disk/sphere for $0 < \rho < R_2 - r$ and partially intersects it for $R_2 - r < \rho < R_1$. Both $g_1(\rho, r)$ and $g_2(\rho, r)$ are used¹.
- **Interval III** ($R_2 < r < R_+$): The ring or shell lies outside the disk/sphere for $0 < \rho < r - R_2$ (probability = 0) and partially intersects it for $r - R_2 < \rho < R_1$. The function $g_2(\rho, r)$ is used¹.

In Table I, we denote $R_- = R_2 - R_1$ and $R_+ = R_1 + R_2$. Moreover, for the 2D case, we define $g_3(\rho, r) = \sqrt{(r^2 - (R_2 - \rho)^2)((R_2 + \rho)^2 - r^2)}$ and $g_4(\rho, r) = \rho^2 + r^2 - R_2^2$. For the 3D case, the corresponding functions are $g_3(\rho, r) = \rho^2 + r^2 - R_2^2$, $g_4(\rho, r) = 13r^2 - 21R_2^2 + 13\rho^2$ and $g_5(\rho, r) = (r - \rho + R_2)^2(\rho - r + R_2)^2$. The closed-form expressions of $f_r(r)$ for the 2D and 3D cases are provided in Theorems 1 and 2, respectively. Furthermore, the special cases $R_1 = R_2 = R$ are delineated as corollaries.

III. INTERNODAL DISTANCE DISTRIBUTIONS

A. 2D networks

Theorem 1. The PDF expression for the internodal distance distribution, r , in a 2D network with $R_1 < R_2$, is given by

$$f_r(r) = \begin{cases} \frac{2rq_1(r)}{R_2^2}, & 0 \leq r < R_-, \\ \frac{r}{2\pi R_1 R_2^2} \left(q_2(r) \arccos\left(\frac{k_1(r)}{2rR_1}\right) + q_3(r) \arccos\left(\frac{k_2(r)}{2rR_2}\right) + q_4(r) \right), & R_- \leq r \leq R_+, \end{cases} \quad (2)$$

where $k_1(r) = r^2 + R_1^2 - R_2^2$ and $k_2(r) = r^2 - R_1^2 + R_2^2$ are system dependent parameters and the polynomials $q_1(r) - q_4(r)$ are specified for each Scenario and tabulated in Table III.

¹As defined in Table II for 2D and Table V for 3D.

Proof:

s2 and s3: The joint PDF of node 2's position under the RWP model, within a circular disk of radius R_2 , centered at $(0, 0)$, with respect to a shifted point at $(\rho, 0)$, is expressed in polar coordinates as

$$f_{r,\vartheta}(r, \vartheta) = \frac{2r}{\pi R_2^2} \left(1 - \frac{r^2 + \rho^2 - 2r\rho \cos\vartheta}{R_2^2} \right). \quad (3)$$

Considering the general equation of a circle, in polar coordinates, centered at $(\rho, 0)$, the angle ϑ can be obtained as

$$\vartheta(r) = \arccos\left(\frac{r^2 - R_2^2 + \rho^2}{2r\rho}\right). \quad (4)$$

Consequently, the conditional PDF of the internodal distance, given that node 1 is located at $(\rho, 0)$, is obtained by integrating (3) over $\vartheta(r)$ in two distinct branches. In the first branch integration is performed over the interval $[0, 2\pi]$ whereas in the second branch, it is carried out over $[-\vartheta(r), \vartheta(r)]$. The final expression can be obtained as

$$f_{r/\rho}(r/\rho) = \begin{cases} g_1(\rho, r), & 0 \leq r < R_2 - \rho \\ g_2(\rho, r), & R_2 - \rho \leq r \leq R_2 + \rho, \end{cases} \quad (5)$$

where $g_1(\rho, r)$, $g_2(\rho, r)$ are presented in Table II.

s1 and s4: The joint PDF remains invariant to the displacement of the center when node 2 is uniformly distributed within a circular region of radius R_2 . That is,

$$f_{r,\vartheta}(r, \vartheta) = \frac{r}{\pi R_2^2}. \quad (6)$$

The conditional PDF of r is derived by integrating (6) over $\vartheta(r)$ in two branches: $[0, 2\pi]$ for the first, and $[-\vartheta(r), \vartheta(r)]$ for the second. Finally, an equivalent expression to (5) is derived, where $g_1(\rho, r)$ and $g_2(\rho, r)$ take distinct values, as shown in Table II. Note that the last two branches (Interval II, III) yield the same result. ■

Corollary 1. The PDF of r for $R_1 = R_2 = R$ is given by

$$f_r(r) = \frac{2r(s_1(r) \arccos(\frac{r}{2R}) + s_2(r) \sqrt{1 - (\frac{r}{2R})^2})}{R^4}, \quad 0 \leq r < 2R, \quad (7)$$

where $s_1(r)$ and $s_2(r)$ are listed in Table IV for each scenario.

Proof: The result follows directly by substituting $R_1 = R_2 = R$ into (2). ■

B. 3D networks

Theorem 2. The PDF expression for the internodal distance distribution, r , in a 3D network with $R_1 < R_2$, is given by

$$f_r(r) = \begin{cases} \sum_{n=1}^3 a_{2n} r^{2n}, & 0 \leq r < R_- \\ \sum_{n=1}^{13} b_n r^n, & R_- \leq r \leq R_+. \end{cases} \quad (8)$$

where a_{2n} and b_n are listed in Tables VI, VIII and IX for each scenario, whereas $b_8 = b_{10} = b_{12} = 0$.

TABLE I
DEFINITION OF r AND ρ INTERVALS FOR THE 2D AND 3D CASES.

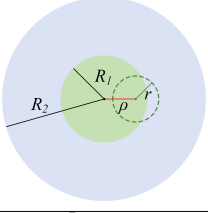
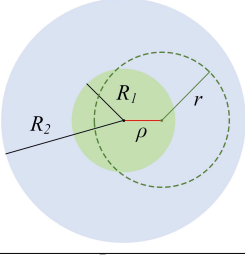
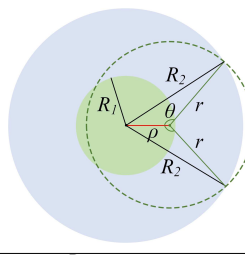
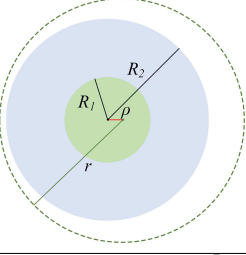
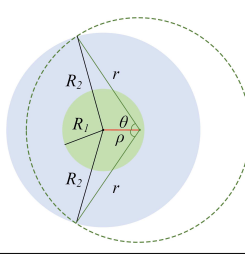
Interval I: $0 < r < R_-$	Interval II: $R_- < r < R_2$		Interval III: $R_2 < r < R_+$	
$0 < \rho < R_1$	$0 < \rho < R_2 - r$	$R_2 - r < \rho < R_1$	$0 < \rho < r - R_2$	$r - R_2 < \rho < R_1$
				
$f_r(r) = \int_0^{R_1} g_1(\rho, r) f_\rho(\rho) d\rho$	$f_r(r) = \int_0^{R_2-r} g_1(\rho, r) f_\rho(\rho) d\rho + \int_{R_2-r}^{R_1} g_2(\rho, r) f_\rho(\rho) d\rho$		$f_r(r) = \int_{r-R_2}^{R_1} g_2(\rho, r) f_\rho(\rho) d\rho$	

TABLE II
DEFINITION OF $g_1(\rho, r)$, $g_2(\rho, r)$ AND $f_\rho(\rho)$ FOR THE 2D CASE.

Function	s1, s4	s2, s3
$g_1(\rho, r)$	$\frac{2r}{R_2^2}$	$-\frac{4r g_4(\rho, r)}{R_2^2}$
$g_2(\rho, r)$	$\frac{2r \arccos\left(\frac{g_4(\rho, r)}{2\rho r}\right)}{\pi R_2^2}$	$\frac{4r(g_3(\rho, r) - g_4(\rho, r) \arccos(\frac{g_4(\rho, r)}{2\rho r}))}{\pi R_2^4}$
Function	s1, s3	s2, s4
$f_\rho(\rho)$	$\frac{4\rho}{R_1^2} \left(1 - \frac{\rho^2}{R_1^2}\right)$	$\frac{2\rho}{R_1^2}$

TABLE III
DEFINITION OF $q_1(r) - q_4(r)$ FOR THE 2D CASE.

	s1	s3
$q_1(r)$	1	$-\frac{2(3r^2 + R_1^2 - 3R_2^2)}{3R_2^2}$
$q_2(r)$	$4R_1^4$	$-\frac{24R_1^4(3r^2 + R_1^2 - 3R_2^2)}{9R_2^2}$
$q_3(r)$	$4R_2^2(2R_1^2 - 2r^2 - R_2^2)$	$-\frac{24R_2^2(3r^2 + R_2^2 - 3R_1^2)}{9}$
$q_4(r)$	$(r^2 - 3R_1^2 + 5R_2^2)g_3(R_1, r)$	$\frac{2g_3(R_1, r)}{9R_2^2} \times (-r^4 + 8r^2(R_1^2 + R_2^2) + 17(R_1^4 + R_2^4) - 22R_1^2 R_2^2)$
	s2	s4
$q_1(r)$	$-\frac{2r^2 + R_1^2 - 2R_2^2}{R_2^2}$	1
$q_2(r)$	$-\frac{4R_1^4(2r^2 + R_1^2 - 2R_2^2)}{R_2^2}$	$4R_1^4$
$q_3(r)$	$4R_1^2 R_2^2$	$4R_1^2 R_2^2$
$q_4(r)$	$\frac{R_1^2(r^2 + 5R_1^2 - 3R_2^2)g_3(R_1, r)}{R_2^2}$	$-4R_1^2 \left(\frac{R_1 k_1(r)}{2r} \sqrt{1 - \left(\frac{k_1(r)}{2r R_1}\right)^2} + \frac{R_2 k_2(r)}{2r} \sqrt{1 - \left(\frac{k_2(r)}{2r R_2}\right)^2} \right)$

Proof:

s2 and s3: The joint PDF for node 2's position under the RWP model, within a sphere of radius R_2 centered at $(0, 0, 0)$, with respect to a shifted point at $(0, 0, \rho)$, is expressed in spherical

TABLE IV
DEFINITION OF $s_1(r)$ AND $s_2(r)$ FOR THE 2D CASE.

	s1, s2	s3	s4
$s_1(r)$	$\frac{2(-r^2 + R^2)}{\pi}$	$\frac{4(-3r^2 + 2R^2)}{3\pi}$	$\frac{2R^2}{\pi}$
$s_2(r)$	$\frac{r(r^2 + 2R^2)}{2\pi R}$	$\frac{-r^5 + 16r^3 R^2 + 12r R^4}{9\pi R^3}$	$-\frac{r R}{\pi}$

TABLE V
DEFINITION OF $g_1(\rho, r)$, $g_2(\rho, r)$ AND $f_\rho(\rho)$ FOR THE 3D CASE.

Function	s1, s4	s2, s3
$g_1(\rho, r)$	$\frac{3r^2}{R_2^2}$	$\frac{35r^2(104\rho^2 r^2 + 6g_3(\rho, r)g_4(\rho, r))}{432R_2^2}$
$g_2(\rho, r)$	$\frac{3r^2}{2R_2^3} \left(1 - \frac{g_3(\rho, r)}{2\rho r}\right)$	$\frac{35r(25R_2^2 - 13(r - \rho)^2)g_5(\rho, r)}{864R_2^2 \rho}$
Function	s1, s3	s2, s4
$f_\rho(\rho)$	$\frac{35}{72} \left(\frac{21\rho^2}{R_1^3} - \frac{34\rho^4}{R_1^5} + \frac{13\rho^6}{R_1^7} \right)$	$\frac{3\rho^2}{R_1^3}$

coordinates as

$$f_{r, \vartheta, \varphi}(r, \vartheta, \varphi) = \frac{35r^2 \sin \vartheta}{288\pi} \left(\frac{21}{R_2^3} - \frac{34(r^2 + \rho^2 - 2r\rho \cos \vartheta)}{R_2^5} + \frac{13(r^2 + \rho^2 - 2r\rho \cos \vartheta)^2}{R_2^7} \right). \quad (9)$$

Considering the general equation of a sphere, centered at $(0, 0, \rho)$, the angle ϑ can be obtained as in (4). The conditional PDF of r , given that node 1 is located at $(0, 0, \rho)$ is obtained by integrating $f_{r, \vartheta, \varphi}(r, \vartheta, \varphi)$ over $\varphi \in [0, 2\pi]$, and ϑ in two branches: $[0, \pi]$ for the first, and $[0, \vartheta(r)]$ for the second. The resulting expression retains the same form as (5); however, in this case, the functions $g_1(\rho, r)$ and $g_2(\rho, r)$ are provided in Table V.

s1 and s4: The joint PDF remains invariant to the displacement of the center when node 2 is uniformly distributed within a sphere with radius R_2 . That is,

TABLE VI
DEFINITION OF a_{2n} FOR THE 3D CASE.

	s1, s4	s2	s3
a_2	$\frac{3}{R_2^3}$	$\frac{65R_1^4 - 238R_1^2R_2^2 + 245R_2^4}{24R_2^7}$	$\frac{35(2275R_1^4 - 11594R_1^2R_2^2 + 18711R_2^4)}{64152R_2^7}$
a_4	0	$\frac{35(13R_1^4 - 17R_2^4)}{36R_2^7}$	$\frac{35(2015R_1^4 - 4131R_2^4)}{8748R_2^7}$
a_6	0		$\frac{455}{72R_2^7}$

TABLE VII
DEFINITION OF c_n FOR THE 3D CASE.

	s1, s2	s3	s4
c_2	$\frac{3}{R^3}$	$\frac{41090}{8019R^3}$	$\frac{3}{R^3}$
c_3		0	$-\frac{9}{4R^4}$
c_4	$-\frac{35}{18R^5}$	$-\frac{18515}{2187R^5}$	0
c_5	$-\frac{35}{16R^6}$	$\frac{1225}{972R^6}$	$\frac{3}{16R^6}$
c_6	$\frac{455}{144R^7}$	$\frac{455}{72R^7}$	0
c_7	$-\frac{287}{288R^8}$	$-\frac{82565}{23328R^8}$	0
c_9	$\frac{65}{2304R^{10}}$	$\frac{1085}{3456R^{10}}$	0
c_{11}	0	$-\frac{7735}{373248R^{12}}$	0
c_{13}	0	$\frac{29575}{49268736R^{14}}$	0

$$f_{r,\vartheta,\varphi}(r, \vartheta, \varphi) = \frac{3r^2 \sin \vartheta}{4\pi R_2^3}. \quad (10)$$

The conditional PDF of the internodal distance is obtained by integrating (10) over $\vartheta(r)$ in two branches: $[0, \pi]$ for the first, and $[0, \vartheta(r)]$ for the second. Finally, an equivalent mathematical expression to (5) is derived, where $g_1(\rho, r)$ and $g_2(\rho, r)$ take distinct values, as shown in Table V. Note that the last two branches (Interval II, III) yield the same result. ■

Corollary 2. The PDF of r for $R_1 = R_2 = R$ is given by

$$f_r(r) = \sum_{n=2}^{13} c_n r^n, 0 \leq r < 2R, \quad (11)$$

where c_n are listed in Table VII for each scenario, whereas $c_8 = c_{10} = c_{12} = 0$.

Proof: The result follows directly by substituting $R_1 = R_2 = R$ into (8). ■

C. Approximation with Beta Distributions

If the presented analytical expressions are deemed too intricate for the direct evaluation of network metrics, tractable approximation techniques may be employed. A commonly adopted approach is to approximate distance-related distributions using a beta distribution. The PDF of the beta distribution is defined as [8]

$$f_x(x) = \frac{x^{\alpha-1}(1-x)^{\beta-1}}{B(\alpha, \beta)}, \quad (12)$$

where α and β are the distribution parameters, and $B(\alpha, \beta)$ is the beta function. The parameters used for the approximation are obtained by matching the first and second moments of the target distribution with those of the beta distribution [8]. Solving the resulting system yields the corresponding optimal parameter values.

Figures 1 and 2 illustrate representative PDF plots for the 2D and 3D cases with $R_2/R_1 = 2$, alongside Monte Carlo simulations. The strong agreement among the simulation histograms, analytical curves, and beta-based approximations confirms the accuracy of the theoretical analysis and validates the derived expressions.

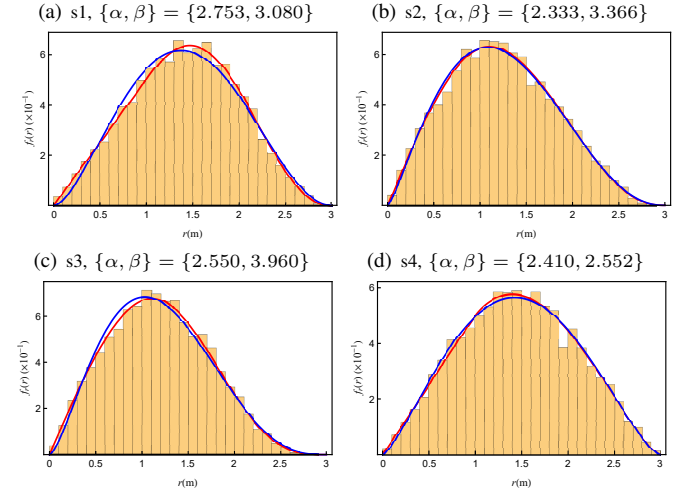


Fig. 1. PDF for the 2D case with $\{R_1, R_2\} = \{1, 2\}m$: analytical solutions (red), beta approximations (blue), and Monte Carlo results (histogram)..

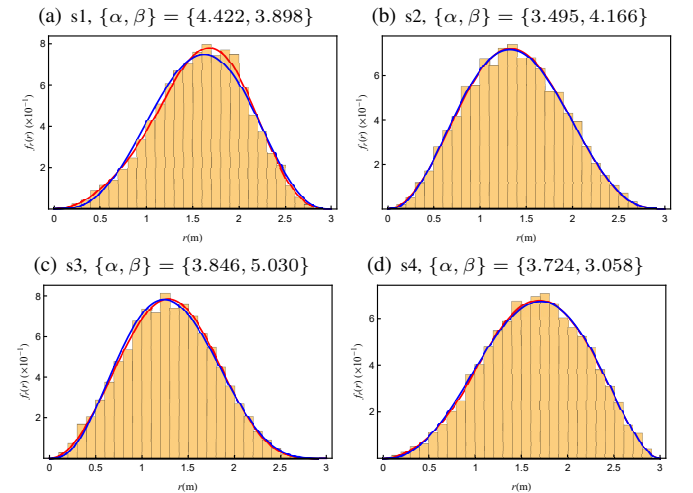


Fig. 2. PDF plots for the 3D case with $\{R_1, R_2\} = \{1, 2\}m$: analytical solutions (red), beta approximations (blue), and Monte Carlo results (histogram).

IV. CONCLUSIONS

This letter introduced a unified analytical framework for the internodal distance distribution in 2D and 3D wireless networks, where nodes are confined to concentric circular or spherical regions. Closed-form PDF expressions were derived for all four node-pair combinations (static-static,

TABLE VIII
DEFINITION OF COEFFICIENTS b_n FOR S1, S2, AND S4 (3D CASE).

	s1	s2	s4
b_1	$\frac{35(29R_1^2 - 13R_2^2)(R_2^2 - R_1^2)^3}{2304R_1^7R_2^3}$	$\frac{35(13R_1^2 - 29R_2^2)(R_2^2 - R_1^2)^3}{2304R_1^7R_2^3}$	$\frac{9(R_2^2 - R_1^2)^2}{16R_1^3R_2^3}$
b_2	$\frac{72R_1^7 + 245R_1^4R_2^3 - 238R_1^2R_2^5 + 65R_2^7}{48R_1^7R_2^3}$	$\frac{72R_2^7 + 245R_2^4R_1^3 - 238R_2^2R_1^5 + 65R_1^7}{48R_1^7R_2^3}$	$\frac{3(R_1^3 + R_2^3)}{2R_1^3R_2^3}$
b_3	$\frac{35(R_2^2 - R_1^2)(25R_1^4 + 88R_1^2R_2^2 - 65R_2^4)}{576R_1^7R_2^3}$	$\frac{35(R_2^2 - R_1^2)(65R_1^4 - 25R_2^4 - 88R_2^2R_1^2)}{576R_1^7R_2^3}$	$\frac{9(R_1^2 + R_2^2)}{8R_1^3R_2^3}$
b_4	$\frac{35(13R_2^2 - 17R_1^2)}{72R_1^7}$	$\frac{35(13R_1^2 - 17R_2^2)}{72R_2^7}$	0
b_5	$\frac{35(7R_1^4 + 34R_1^2R_2^2 - 65R_2^4)}{384R_1^7R_2^3}$	$\frac{35(7R_2^4 + 34R_2^2R_1^2 - 65R_1^4)}{384R_1^7R_2^3}$	$\frac{3}{16R_1^3R_2^3}$
b_6	$\frac{455}{144R_1^7}$	$\frac{455}{144R_2^7}$	0
b_7	$-\frac{7(17R_1^2 + 65R_2^2)}{576R_1^7R_2^3}$	$-\frac{7(17R_2^2 + 65R_1^2)}{576R_1^7R_2^3}$	0
b_9	$\frac{65}{2304R_1^7R_2^3}$	$\frac{65}{2304R_1^7R_2^3}$	0
b_{11}	0	0	0
b_{13}	0	0	0

TABLE IX
DEFINITION OF COEFFICIENTS b_n FOR S3 (3D CASE).

	s3
b_1	$\frac{245(R_2^2 - R_1^2)^4(1442R_1^2R_2^2 - 481(R_1^4 + R_2^4))}{1492992R_1^7R_2^7}$
b_2	$\frac{35(2275(R_1^4 + R_2^4) - 11594(R_1^3R_2^2 + R_1^2R_2^3) + 18711(R_1^2R_2^4 + R_1^4R_2^2))}{128304R_1^7R_2^7}$
b_3	$\frac{1225(R_2^2 - R_1^2)^2(R_1^4 + R_2^4)(350R_1^2R_2^2 - 143(R_1^4 + R_2^4))}{82944R_1^7R_2^7}$
b_4	$\frac{35(2015(R_1^3 + R_2^3) - 4131(R_1^2R_2^2 + R_1^4R_2^2))}{17496R_1^7R_2^7}$
b_5	$\frac{1225(1700(R_1^6R_2^2 + R_1^2R_2^6) + 882R_1^4R_2^4 - 1885(R_1^8 + R_2^8))}{497664R_1^7R_2^7}$
b_6	$\frac{455(R_1^4 + R_2^4)}{144R_1^7R_2^7}$
b_7	$\frac{245(R_1^2 + R_2^2)(554R_1^2R_2^2 - 1625(R_1^4 + R_2^4))}{373248R_1^7R_2^7}$
b_9	$\frac{35(455(R_1^4 + R_2^4) - 788R_1^2R_2^2)}{165888R_1^7R_2^7}$
b_{11}	$-\frac{7735(R_1^4 + R_2^4)}{746496R_1^7R_2^7}$
b_{13}	$\frac{29575}{49268736R_1^7R_2^7}$

static–mobile, mobile–static, and mobile–mobile) under both uniform and random waypoint spatial models, including the important special case of equal radii. The derived distance distributions enable a tractable evaluation of connectivity, coverage, outage, interference, and hop-count statistics without resorting exclusively to time-consuming simulations and they can be readily embedded into higher-layer models for routing, power control, and resource allocation. Future work may consider extending the proposed framework to alternative mobility models and to non-concentric or irregular deployment regions.

REFERENCES

- [1] D. Moltchanov, “Distance distributions in random networks,” *Ad Hoc Netw.*, vol. 10, no. 6, pp. 1146–1166, 2012.
- [2] J. Yick, B. Mukherjee, and D. Ghosal, “Wireless sensor network survey,” *Comput. Netw.*, vol. 52, no. 12, pp. 2292–2330, 2008.
- [3] M. Haenggi, *Stochastic Geometry for Wireless Networks*. New York, USA: Cambridge Univ. Press, 2012.
- [4] A. Talgat, M. A. Kishk, and M.-S. Alouini, “Nearest neighbor and contact distance distribution for binomial point process on spherical surfaces,” *IEEE Commun. Lett.*, vol. 24, no. 12, pp. 2659–2663, Dec. 2020.
- [5] N. Okati, T. Riihonen, D. Korpi, I. Angervuori, and R. Wichman, “Downlink coverage and rate analysis of low earth orbit satellite constellations using stochastic geometry,” *IEEE Trans. Commun.*, vol. 68, no. 8, pp. 5120–5134, Aug. 2020.
- [6] N. Vaipoulos, A. Vavoulas, and H. G. Sandalidis, “Exploring the random location problem inside a truncated conic shape: Application in UAV communications,” *IEEE Trans. Commun.*, vol. 70, no. 4, pp. 2882–2890, Apr. 2022.
- [7] N. Vaipoulos, A. Vavoulas, H. E. Nistazakis, H. G. Sandalidis, and A. Kakarountas, “On the UOWC performance under location uncertainty,” *IEEE Access*, vol. 11, pp. 38 783–38 794, 2023.
- [8] N. Y. Ermolova and O. Tirkkonen, “Using beta distributions for modeling distances in random finite networks,” *IEEE Commun. Lett.*, vol. 20, no. 2, pp. 308–311, Feb. 2015.
- [9] J. Nichols and J. Michalowicz, “Distance distribution between nodes in a 3D wireless network,” *J. Parallel Distrib. Comput.*, vol. 102, pp. 71–79, 2017.
- [10] E. Hyttia, P. Lassila, and J. Virtamo, “Spatial node distribution of the random waypoint mobility model with applications,” *IEEE Trans. Mobile Comput.*, vol. 5, no. 6, pp. 680–694, Jun. 2006.
- [11] X. Zhong, F. Chen, Q. Guan, F. Ji, and H. Yu, “On the distribution of nodal distances in random wireless ad hoc network with mobile node,” *Ad Hoc Netw.*, vol. 97, p. 102026, 2020.
- [12] J. P. Mullen, “Robust approximations to the distribution of link distances in a wireless network occupying a rectangular region,” *ACM SIGMOBILE Mob. Comput. Commun. Rev.*, vol. 7, no. 2, pp. 80–91, 2003.
- [13] A. M. Mathai, *An Introduction to Geometrical Probability: Distributional Aspects with Applications*. Amsterdam, The Netherlands: Gordon & Breach, 1999.
- [14] C. Bettstetter, “Topology properties of ad hoc networks with random waypoint mobility,” *Mob. Comput. Commun. Rev.*, vol. 7, no. 3, pp. 50–52, 2003.
- [15] M. Parry and E. Fischbach, “Probability distribution of distance in a uniform ellipsoid: Theory and applications to physics,” *J. Math. Phys.*, vol. 41, no. 4, pp. 2417–2433, 2000.